NASA TECHNICAL TRANSLATION NASA TT F-15,012

EXPERIMENTAL DETERMINATION OF BOUND VORTEX LINES AND FLOW IN THE VICINITY OF THE TRAILING EDGE OF A SLENDER DELTA WING

D. Hummel and G. Redeker

Translation of "Experimentelle Bestimmung der gebundenen Wirbellinien sowie des Strömungsverlaufs in der Umgebung der Hinterkante eines schlanken Deltaflügels," Braunschweigische Wissenschaftliche Gesellschaft, Abhandlungen, 1972, pp. 273-290

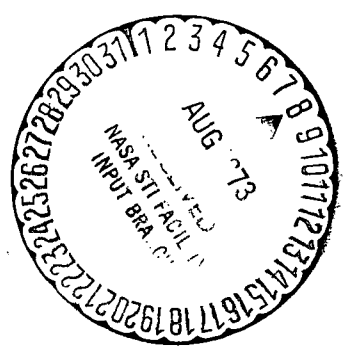

NATIONAL AERONAUTICS AND SPACE ADMINISTRATION
WASHINGTON, D. C. 20546 AUGUST 1973

STANDARD TITLE PAGE

1. Report No. NASA TT F-15,012	2. Government Accession No.	3. Recipient's Catalog No.
4. Title and Subtitle EXPERIMENTAL DETERMINATION OF BOUND VORTEX LINES AND FLOW IN THE VICINITY OF THE TRAILING EDGE OF A SLENDER DELTA WING		5. Report Date August 1973 6. Performing Organization Code
7. Author(s) D. Hummel and G. Redeker		8. Performing Organization Report No. 10. Work Unit No.
9. Performing Organization Name and Address Leo Kanner Associates Redwood City, California 94063		11. Contract or Grant No. NASw-2481 13. Type of Report and Period Covered Translation
12. Sponsoring Agency Name and Address National Aeronautics and Space Administration, Washington, D. C. 20546		14. Sponsoring Agency Code

15. Supplementary Notes

Translation of "Experimentelle Bestimmung der gebundene Wirbellinien sowie des Strömungsverlaufs in der Umgebung der Hinterkante eines schlanken Deltaflügels," Braunschweigische Wissenschaftliche Gesellschaft, Abhandlungen, 1972, pp. 273-290

16. Abstract Boundary layer measurements have been carried out on a sharp-edged delta wing (Aspect ratio A = 1.0, angle of incidence α = 20.5°) with turbulent boundary layers. From the velocities at the outer edge of the boundary layer on the upper and the lower side of the wing the bound vortex lines in the lifting surface were determined. A comparison with former investigations concerning laminar boundary layers shows the influence of the status of the boundary layer on vortex formation. Studies on the flow downstream from the wing trailing-edge indicate that the trailing vortex sheet rolls up into a vortex, the rotation of which is opposite to that of the leading-edge vortex. The axis of this so-called trailing-edge vortex forms a spiral within the leading-edge vortex.

17. Key Words (Selected by Author(s))	18. Distribution Statement Unclassified-Unlimited		
19. Security Classif. (of this report) Unclassified	20. Security Classif. (of this page) Unclassified	21. No. of Pages 23	22. Price

EXPERIMENTAL DETERMINATION OF BOUND VORTEX LINES AND FLOW IN THE VICINITY OF THE TRAILING EDGE OF A SLENDER DELTA WING

Dietrich Hummel and Günter Redeker
Institut für Aerodynamik of the Deutsche Forschungs- und Versuchsanstalt für Luft- und Raumfahrt (DFVLR), Braunschweig

1. Introduction

/273*

Even at small angles of attack, flow separates at the leading edges of slender, sharp-edged wings, and two concentrated vortices are generated above the wing. These have a very pronounced effect on flow at the wing, particularly pressure distribution over the upper surface. A nonlinear relationship is found between the lift coefficient for the wing and the angle of attack, typical of slender wings. Fig. 1 shows a schematic representation of these conditions.

A number of methods have been developed for calculating the nonlinear component of the lift of such wings (cf. [1]), based on different assumptions. In the articles by C. E. Brown, W. H. Michael [2], K. W. Mangler, J. H. B. Smith [3] and J. H. B. Smith [4], attempts are made to theoretically characterize vortical flow over the wing as well as possible. This only succeeds in cases restricted to conical flow, so Kutta's flow-off condition is violated at the trailing edge. The methods of D. Kücheman [5] and K. Gersten [6] work with extreme simplification of the flow actually occurring at the wing; however, they do satisfy Kutta's flow-off condition. Recently, R. K. Nangia, G. J. Hancock [7] made an attempt to link the two different approaches in nonlinear wing theory together. The satisfaction of Kutta's flow-off condition was incorporated into Brown and Michael's method [2] in the process.

/274

* Numbers in the margin indicate pagination in the foreign text.

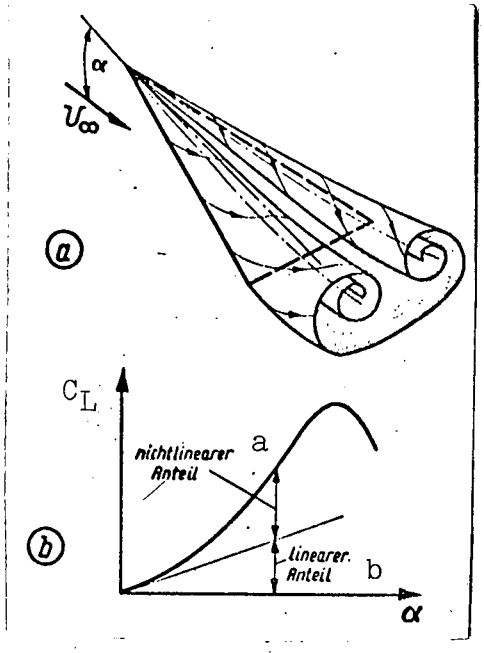

Fig. 1. Flow around and lift behavior of a slender wing (schematic). a) vortex formation. b) lift characteristic $C_L(\alpha)$.

Key: a. Nonlinear component; b. Linear component

Additional improvements in the nonlinear theory are likely to be possible only on the basis of exact knowledge of actual flow conditions. In particular, this includes the path of bound vortex lines on the wing and of free vortices over and downstream from the wing. Flow around sharp-edged slender wings is very well known on the basis of a large number of experimental studies, cf. [8-10]. Qualitative studies by B. J. Elle, J. P. Jones [11] are available on the vortical system which occurs in the flow.

For some time now, work has been going on at the Institut für Aerodynamik of the DFVLR to quantitatively determine, experimentally, the system of bound and free vortex lines on a delta wing of very small aspect ratio. The behavior of bound vortex lines in the lifting surface was first determined here from the velocity difference between the upper and the lower wing surfaces. D. Hummel [12] has reported on the results of these measurements. /275 These studies were carried out at a Reynold's number of $Re = U_\infty \ell_i/\nu = 9 \cdot 10^5$, so laminar boundary layers existed on the wing. Since considerable differences between measured pressure distribution on the upper surface of the wing and that calculated by J. H. B. Smith's method [4] were found in this case, corresponding studies with artificially turbulent boundary layers on the upper surface of the wing were carried out in the first part of the present work in order to determine the effect of boundary-

layer character on the behavior of bound vortex lines. The earlier studies [12] showed behavior on the part of bound vortex lines in the vicinity of the trailing edge which indicated that the free vortex lines leaving the trailing edge of the wing must have a direction of rotation opposed to that of the principal vortex. These conditions in the vicinity of the trailing edge were studied qualitatively in a water tunnel in the second part of this work in order to obtain preliminary data on the behavior of free vortices downstream from the trailing edge.

The actual quantitative determination of free vortex lines over and downstream from the wing has yet to be accomplished. A second report on the status of these studies is given in this article.

2. Notation

2.1. Geometric Quantities

x, y, z	Coordinate system fixed relative to wing, with origin at nose of wing as shown in Fig. 2
$\underline{i}, \underline{j}$	Unit vectors in x- and y-directions
b	Wing span
S	Wing area
$\ell(y)$	Local chord length
$s(x)$	Local half-span
A	Aspect ratio ($= b^2/S$)
η	Dimensionless coordinate referred to local half-span [$\eta = y/s(x)$]
D	Diameter of turbulence filaments

2.2. Aerodynamic Quantities

U_∞	Oncoming flow velocity
$\underline{w}$	Velocity vector at outer margin of boundary layer

	(Components: u, v, w = 0)
$\underline{k}$	Vector of vortex density from Eq. (3) (components: k_x, k_y, k_z = 0)
p	Static pressure
p_∞	Static pressure in oncoming flow
q_∞	Dynamic pressure of oncoming flow [$=(\rho/2)U_\infty^2$]
c_p	Coefficient of static pressure [$= (p - p_\infty)/q_\infty$]
α	Angle of attack
C_L	Lift coefficient ($= L/q_\infty S$)
ρ	Air density
ν	Kinematic viscosity of air
Re	Reynolds number ($= U_\infty \ell_i/\nu$)

2.3. Subscripts

i	Inboard (center airfoil section)
u	Upper side of wing
ℓ	Lower side of wing

3. Overview of the Measurements

/276

3.1. Wind-Tunnel Studies

The measurements were performed on a sharp-edged delta wing with an aspect ratio of A = 1.0 in the 1.3-m wind tunnel of the Institut für Strömungsmechanik of the Technische Universität Braunschweig. The wing model used in shown in Fig. 2. The wing is flat on one side and has a very shallow triangular cross section perpendicular to this plane. Maximum relative thickness is at $x/\ell_i = 0.9$ and is 2.1% of ℓ_i. Pressure-gauge tubes with pressure-sampling holes drilled in them at a large number of points (cf. Fig. 2) are recessed in the surface of the wing on both sides for measuring static pressure.

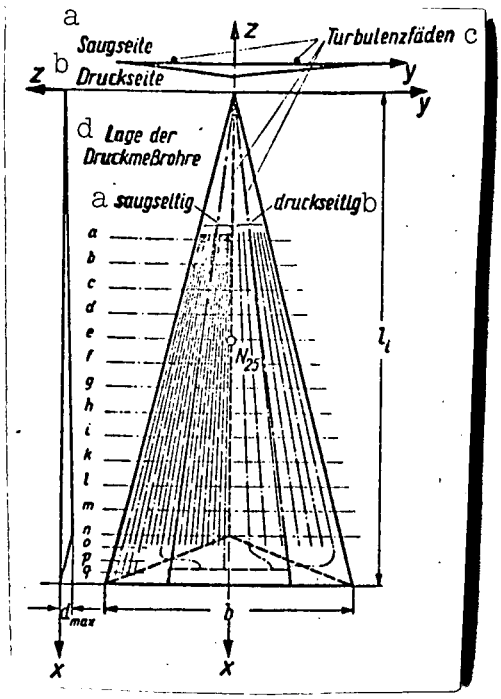

Fig. 2. Delta wing A = 1 for wind-tunnel studies. ℓ_i = = 750 mm, b = 375 mm, d_{max} = = 16 mm (at $x/\ell_i = 0.9$); a through q: sections for measuring pressure distribution; N_{25}: geometric neutral point.

Key: a. Suction side; b. Pressure side; c. Turbulence filaments; d. Location of pressure sampling tubes

Six-component and pressure-distribution measurements on this wing and the behavior of flow on the suction side of this wing have already been reported on [10, 13]. The experimental determination of the behavior of bound vortex lines on that wing at an angle of attack of $\alpha = 20.5°$ was covered in [12]. In those studies, the Reynolds number was $Re = U_\infty \ell_i/\nu = 9 \cdot 10^5$, and the boundary layers were laminar on both sides. The lift characteristic $C_L(\alpha)$ for this wing is shown in [15], Fig. 6. Accordingly, a lift coefficient of C_L = = 0.72 is associated with attack angle $\alpha = 20.5°$, studied here, while the maximum lift coefficient for this wing is C_{Lmax} = = 1.05.

In the present measurements, /277 the wing was likewise studied at an angle of attack of $\alpha = 20.5°$, Reynolds no. $Re = 9 \cdot 10^5$. In this case, however, a turbulent boundary layer is produced artificially on the suction side of the wing with the aid of turbulence filaments (diameter D = 1 mm, position $y/s(x) = \pm 0.5$). The results of the associated preliminary studies are reported in Section 4.1. Pressure distribution over the wing, velocity distribution in the boundary layer, and the behavior of lines of flow at the wall were determined on the suction side and on the pressure side of the wing. For this purpose, : static pressure was measured at the wing surface and

total pressure and flow direction at various distances from the wall; from these were determined the velocity distribution within the boundary layer. The flat side of the wing was used as the suction or pressure side in each case, and the slight camber effect on flow was neglected. The path of wall flow lines was made visible with the aid of a "paint" method. For this purpose, the wing was given a coat of a suspension of aluminum-oxide powder in petroleum and gasoline (mixing ratio 1 g aluminum oxide to 3 cm^3 petroleum and 1 cm^3 gasoline) and was briefly exposed to fluid flow.

The local vortex density vectors on the lifting surface was then determined from the vector difference in the velocities measured at the margin of the boundary layer on the suction and pressure sides. The velocity vectors on the suction and pressure sides of the wing are

$$\begin{aligned} \underline{w}_u &= u_u\underline{i} + v_u\underline{j} \\ \underline{w}_\ell &= u_\ell\underline{i} + v_\ell\underline{j} \end{aligned} \tag{1}$$

For the vector of the velocity difference we thus obtain

$$\begin{aligned} \Delta\underline{w} &= (u_u - u_\ell)\underline{i} + (v_u - v_\ell)\underline{j} \\ \Delta\underline{w} &= \Delta u\ \underline{i} + \Delta v\underline{j}. \end{aligned} \tag{2}$$

The vortex density vector is perpendicular to the velocity difference vector, i.e.

$$\begin{aligned} \underline{k} &= k_x\underline{i} + k_y\underline{j} \\ \underline{k} &= -\Delta v\ \underline{i} + \Delta u\underline{j} \end{aligned} \tag{3}$$

From the directional field of measured vortex density vectors, it is possible to determine the bound vortex lines at the lifting surface by integration. The measurements were evaluated as

described in [12], in such a manner that the secondary vortex on the suction side of the wing was considered to be a phenomenon of boundary-layer flow and was counted as part of the boundary layer.

3.2. Water-Tunnel Studies

The measurements were conducted in the water tunnel of the Institut für Strömungsmechanik of the Technische Universität Braunschweig (measurement cross section 250 x 330 mm). The wing model used in shown in Fig. 3. It has the same plan form as the wind-tunnel model, but a different thickness distribution, with a maximum relative thickness of 2.5% of ℓ_i, at $x/\ell_i = 0.5$. Dye is introduced through the model through notches cut into the surface on the suction side. The suction side of the wing has a foil cemented to it which is pierced at suitable points for the emission of dye into the stream. /278

In these studies, dye was injected into the boundary layers on the upper and lower sides of the wing, and vortex formation was photographed downstream from the trailing edge. Free stream velocity was $U_\infty = 5$ cm/sec. This corresponds to a Reynolds number of $Re = U_\infty \ell_i / \nu = 10^4$.

4. Experimental Determination of Bound Vortex Lines

Comparison of results for laminar and for turbulent boundary layers.

4.1. Preliminary Studies on the Production of Turbulent Boundary Layers

The paths of wall flow lines on the delta wing with A = 1.0 at an angle of attack of $\alpha = 20.5°$ and Reynolds number $Re = 9 \cdot 10^5$

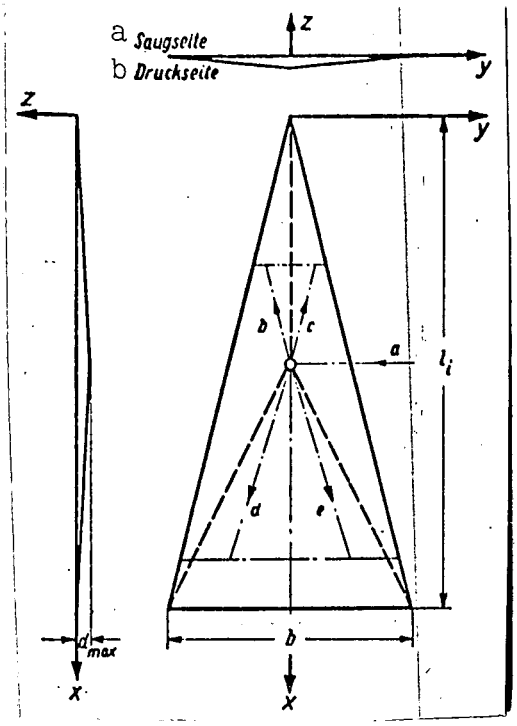

Fig. 3. Delta wing A = 1 for water-tunnel studies. ℓ_i = 200 mm, b = 100 mm, d_{max} = = 5 mm (at $x/\ell_i = 0.5$); a through e: Dye feed lines in the model.

Key: a. Suction side; b. Pressure side.

can be seen from Fig. 4. According to the earlier studies [10], the boundary layers are laminar on the lower side (Fig. 4 a) and on the upper side (Fig. 4 b). The position of the secondary separation line at $\eta = \pm 0.67$ is characteristic of this. Laminar separation is accompanied by a pronounced secondary vortex, and the line of separation is located at a considerable distance from the leading edge. A turbulent boundary layer is accompanied only by a weak secondary vortex, on the other hand, and the line of separation lies closer to the leading edge of the wing. This characteristic of flow on the suction side with a turbulent boundary layer was utilized in the preliminary studies to es- /280 tablish the position and thickness of the turbulence filaments in such a manner that a turbulent boundary layer was generated from the nose of the wing to the trailing edge. The results are shown in Fig. 4 c. Turbulence filaments of 1 mm diameter which were applied at a half half-span $\eta = \pm 0.5$ as shown in Fig. 2 produced turbulent boundary layers over the outboard portion of the wing, $\eta > 0.5$. The secondary separation lines occurred at $\eta = \pm 0.8$ in this case. The remaining boundary layers on the suction side within the interval $-0.5 \leq \eta \leq 0.5$ and on the pressure side were laminar.

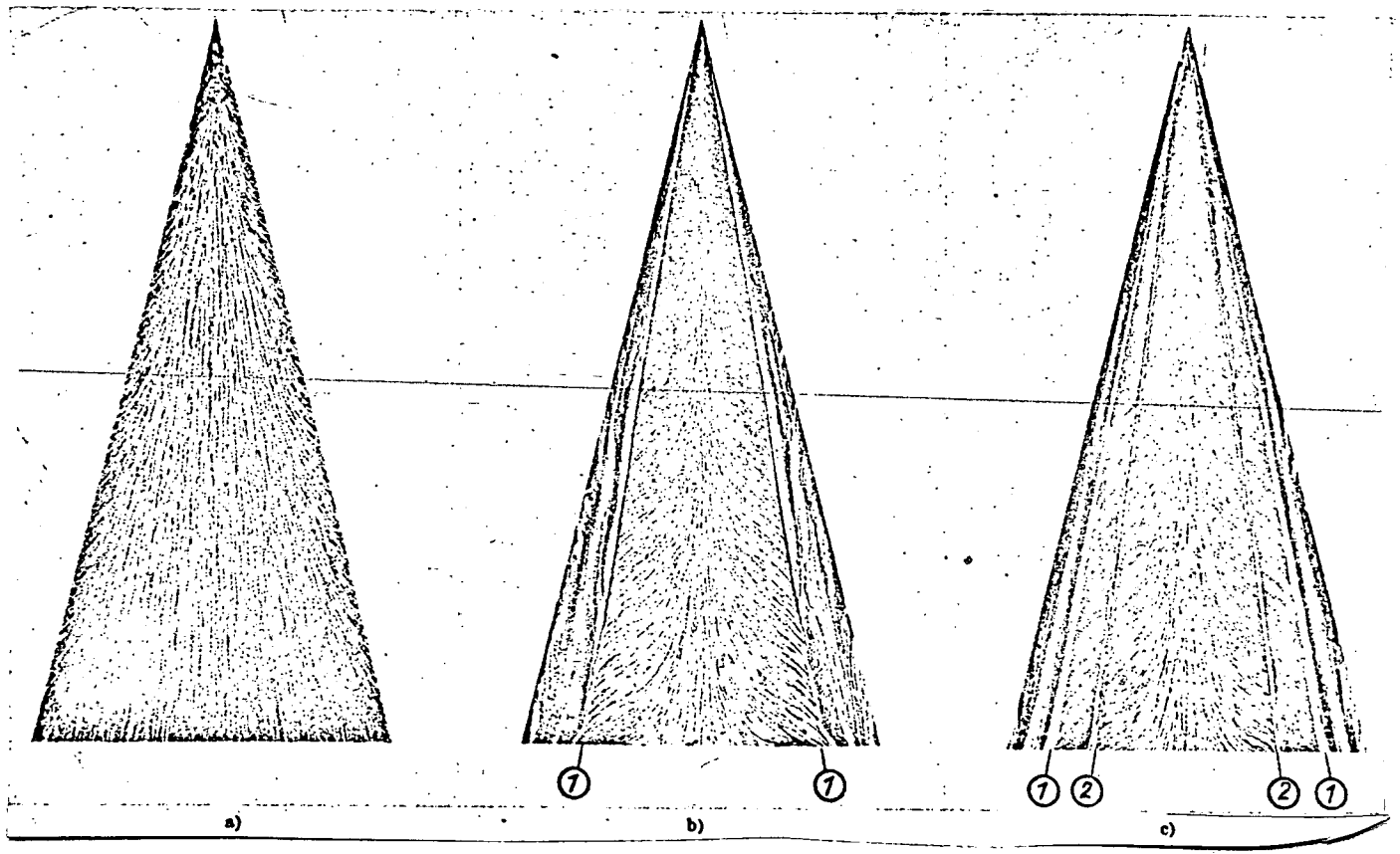

Fig. 4. Paths of wall flow lines on the delta wing A = 1 at α = 20.5°, Re = = $9 \cdot 10^5$. a) Pressure side: boundary layer laminar; b) Suction side: boundary layer laminar; c) Suction side: boundary layer artificially turbulent, turbulence filaments at $\eta = \pm 0.5$; (1) secondary separation line; (2) turbulence filaments. /279

4.2. Pressure Distribution and Secondary Separation

The measured pressure distribution is shown in Fig. 5 for various sections, x/ℓ_i = const., on the pressure and suction sides. The pressure coefficient c_p is plotted against local half-span η in each case. On the pressure side, there is a uniform distribution of overpressures, which fall off in the vicinity of the leading edges. Pronounced underpressures are present on the suction side, which increase sharply in the vicinity of the leading-edge vortex ($\eta \sim 0.7$). At this angle of attack, flow already deviates considerably from conical behavior. Theoretical pressure /281 distributions based on the nonlinear theory of J. H. B. Smith [4] and based on the linear theory of slender bodies of R. T. Jones [14] are plotted for comparison with these measurements. Both theories indicate a conically symmetrical pressure distribution for the delta wing, so the same curve is obtained in each case for all sections. In the forward section at $x/\ell_i = 0.3$, where an approximately conical flow still prevails, agreement between experiment and nonlinear theory is very good, whereas the theory of slender bodies agrees poorly with the measurements, as to be expected.

The pressure distributions measured over the section at $x/\ell_i = 0.3$ with a laminary boundary layer, from [12], and for an artificially turbulent boundary layer are compared with one another in Fig. 6. It is seen here that very much greater underpressures are achieved with the turbulent boundary layer in the vicinity of the leading-edge vortex than with a laminar boundary layer. The underpressure maximum is located at approximately $\eta = 0.61$ for the laminar boundary layer, and at $\eta = 0.68$ for the turbulent boundary layer. It follows from this that the leading-edge vortex lies closer to the leading edge for the turbulent boundary layer. If it is assumed that circulation in the leading- /282 edge vortex is approximately the same in both cases, the suction

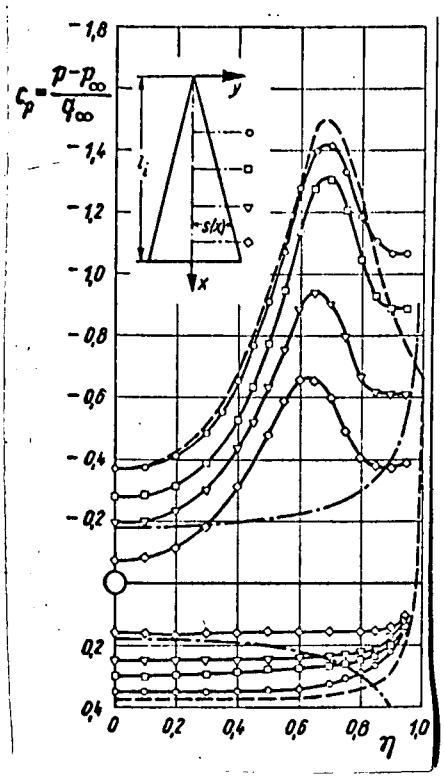

Fig. 5. Pressure distribution over delta wing A = 1 at $\alpha = 20.5°$ with turbulent boundary layer.
Measured at x/ℓ_i = 0.3 -O-
0.5 -□-
0.7 -▽-
0.9 -◇-
Nonlinear theory, J. H. B. Smith [4] ----
Linear theory, R. T. Jones [14] - · - · - ·

[Translator's note: commas in numerals are equivalent to decimal points.]

peak achieved in each case incicates that the leading edge vortex is located at a shorter distance from the upper side of the wing in the case of the turbulent boundary layer than in the case of the laminar boundary layer; cf. Fig. 6 b. Secondary separation occurs within the interval $0.67 \leq \eta \leq 1.0$ for the laminar boundary layer and $0.80 \leq \eta \leq 1.0$ for the turbulent boundary layer. This is in good agreement with the "paint" pictures shown in Fig. 4 b, c. The pressure distributions differ considerably in these ranges. In the laminar boundary layer case, a pronounced secondary vortex is formed which causes considerable additional underpressures on the wing, whereas only a weak secondary vortex with small additional underpressures occurs with the turbulent boundary layer.

Accordingly, secondary-vortex development very strongly affects flow behavior about a delta wing. Apparently, the displacement effect of the secondary flow on the remaining flow field represents the decisive influencing factor here. In contrast to the laminar boundary layer case, the secondary vortex is smaller and its displacement effect weaker for the turbulent boundary layer. As a result, the principal vortex lies closer to the leading edge

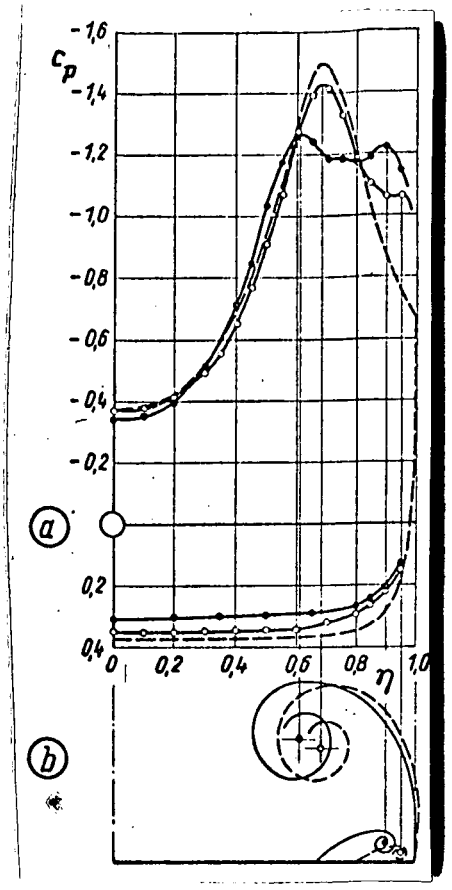

Fig. 6. Pressure distribution and vortex formation on delta wing A = 1 at $\alpha = 20.5°$ at section $x/\ell_i = 0.3$ for laminar and turbulent boundary layers.

a) Pressure distribution
—●— boundary layer laminar [12]
—○— Boundary layer turbulent
----- Theory, J. H. B. Smith [4]

b) Vortex formation (schematic)
——— Boundary layer laminar
----- Boundary layer turbulent

and to the wing. This results in greater underpressures on the suction side of the wing. The agreement between measured pressure distributions and J. H. B. Smith's [4] nonlinear theory, in which secondary vortex formation is not taken into consideration, becomes better the smaller the secondary vortex is.

4.3. Velocity Components at the Margin of the Boundary Layer

The velocity vectors at the outer margin of the boundary layer as measured with a turbulent boundary layer yield a picture similar to that obtained in the measurements with a laminar boundary layer in [12]. The components u/U_∞ are plotted in Fig. 7 and the components v/U_∞ in Fig. 8 for the section $x/\ell_i = 0.3$ in each case to allow the measurements for laminar and turbulent boundary layers to be compared. It is found here that the differences in pressure distribution for laminary and turbulent boundary layers based on Fig. 6 can be attributed to the v components of different magnitude on the suction side.

This situation is a direct consequence of the displacement of the axis of the leading-edge /283

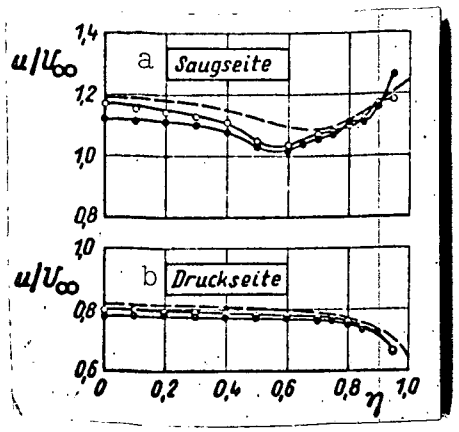

Fig. 7. Velocity components u/U_∞ at the margin of the boundary layer on delta wing A = 1 at $\alpha = 20.5°$ at section $x/\ell_i = 0.3$.
—●— Boundary layer laminar [12]
—O— Boundary layer turbulent
----- Theory, J.H.B. Smith [4].

Key: a. Suction side; b. Pressure side.

vortex relative to the wing described in Section 4.2. A comparison of the measurements with J. H. B. Smith's [4] nonlinear theory indicates that the velocity components u and v agree better with theory for a turbulent boundary layer than for a laminar boundary layer.

4.4. Vortex Density Vectors and Paths of Bound Vortex Lines

The components of the vector of vortex density and thus the magnitudes and directions of the vortex density vectors were determined from the difference in the u and v components of velocity between the suction and pressure sides of the wing. The results are shown in Fig. 9. The vortex density vectors determined from the measurements are drawn into the wing plan in the right half of the diagram. The maximum in vortex density is located at $\eta = 0.7$ in the vicinity of the leading-edge vortex. The directional field of the vortex density vectors describes the behavior of the bound vortex lines at the lifting surface. The vortex density vectors are always directed tangentially to the vortex lines. A high vortex density at one point indicates that the vortex lines there are at small distances from one another, and vice versa. Individual vortex lines were determined by integration over the experimentally determined field of vortex density vectors. The vortex lines passing through points $x_i/\ell_i = 0.4$, 0.6 and 0.9 on the center section are shown as the results in the left half of Fig. 9. A comparison with the associated /284

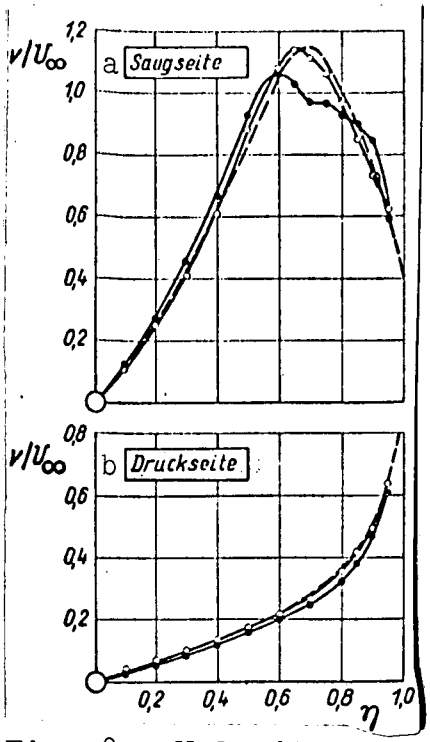

Fig. 8. Velocity components v/U at the margin of the boundary layer on delta wing A = 1 at $\alpha = 20.5°$ at section $x/\ell_i = 0.3$.
—●— Boundary layer laminar [12]
—○— Boundary layer turbulent
----- Theory, J. H. B. Smith [4].

Key: a. Suction side; b. Pressure side

theoretical vortex lines based on J. H. B. Smith's [4] nonlinear theory shows very good agreement in the forward portion of the wing, in which approximately conical flow exists, whereas the difference between theory and experiment increases markedly as the trailing edge of the wing is approached.

The paths of bound vortex lines for laminar and turbulent boundary layers are compared with one another in Fig. 10. The vortex lines through points $x_i/\ell_i = 0.4$, 0.6 and 0.9 are shown. Overall, it is found that the differences in the paths of the vortex lines for laminar and turbulent boundary layers are not very great. In the forward portion of the wing, the vortex lines for a turbulent boundary layer agree somewhat better with J. H. B. Smith's [4] nonlinear theory than those for a laminar boundary layer.

5. Flow Behavior in the Vicinity of the Trailing Edge

5.1. Vortex Lines at the Trailing Edge

The results for vortex density vectors for a laminar boundary layer according to [12] and those for a turbulent layer from Fig. 9 are in agreement to the effect that the measured vortex density vectors $\underline{k}$ have negative x-components along the entire trailing edge. In particular /285

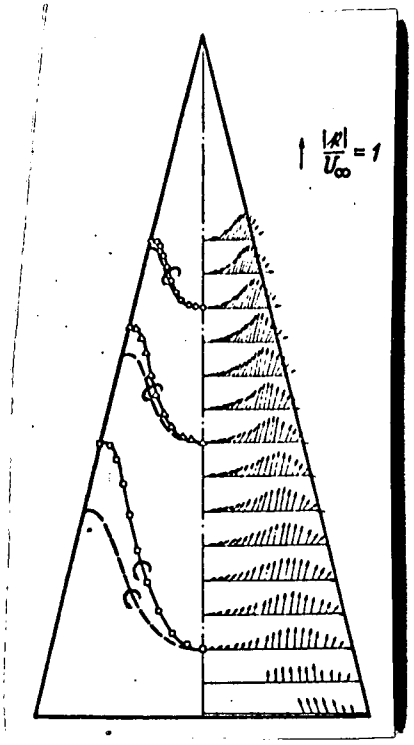

Fig. 9. Vortex density vectors (right side) and paths of the bound vortex lines (left side) on delta wing A = 1 at α = = 20.5° for a turbulent boundary layer. Comparison between theory and measurements.
---- Theory, J. H. B. Smith [4]

$$k_x < 0 \text{ and } k_y > 0$$

at the trailing edge near the center of the wing and thus, according to Eq. (3),

$$v_u > v_\ell \text{ and } u_u > u_\ell;$$

near the outboard edge,

$$k_x < 0 \text{ and } k_y < 0$$

and thus

$$v_u > v_\ell \text{ and } u_u < u_\ell.$$

Fig. 11 shows photographs of the flow about a delta wing of aspect ratio A = 1.0 at angle of attack α = 15° in the water tunnel. In Fig. 11 a, dye is injected into flow over the lower side of the wing and, in Fig. 11 b, over the upper side, close to the trailing edge. Since the magnitudes of velocity over the upper and lower sides are the same at the trailing edge, $|\underline{w}_u| = |\underline{w}_\ell|$, it follows from the different angles of inclination of the flow lines relative to the trailing edge that $v_u > v_\ell$ there. This means that free vortices must leave the trailing edge in the rearward direction, the rotation of which must be opposite to that of the principal vortex over that half of the wing.

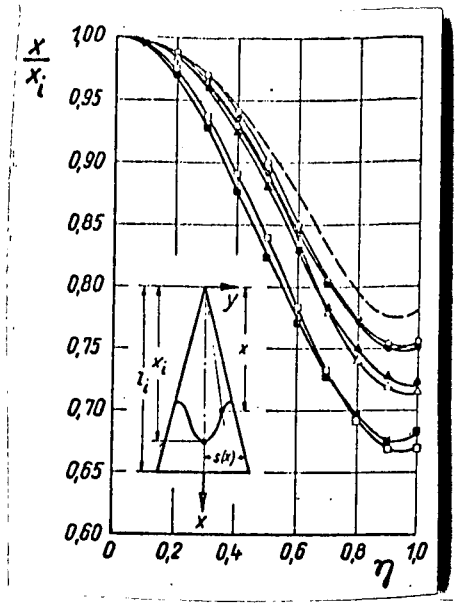

Fig. 10. Paths of bound vortex lines on delta wing $A = 1$ at $\alpha = 20.5°$.

Boundary layer

Paste

---- Theory, J. H. B. Smith [4]

5.2. Vortex Formation Downstream from the Trailing Edge

The basic characteristics of vortex formation behind the wing can likewise be seen from Fig. 11. The leading-edge vortex passing over the wing is characterized by a spiral flow line over and downstream from the wing. Some of the dye exiting on the lower side of the wing ends up in the vortex sheet coming off the leading edge of the wing, as shown in Fig. 11 a. This is thereby made visible in a band. We see a broad band of dye which, in the form of a spiral, curls into the principal vortex. The other portion of the dye injected on the lower side of the wing reaches the trailing edge and leaves the wing in the vortex sheet which originates there. Downstream from the trailing edge, this vortex sheet rolls into a vortex which moves downstream in the approximate form of an extension of the leading edge; its direction of rotation opposes that of the principal vortex. /286

In contrast to the leading-edge vortex(principal or primary vortex) over the wing and the secondary vortex on the wing resulting from instances of boundary-layer separation, this additional vortex will be referred to as the trailing-edge vortex in the following.

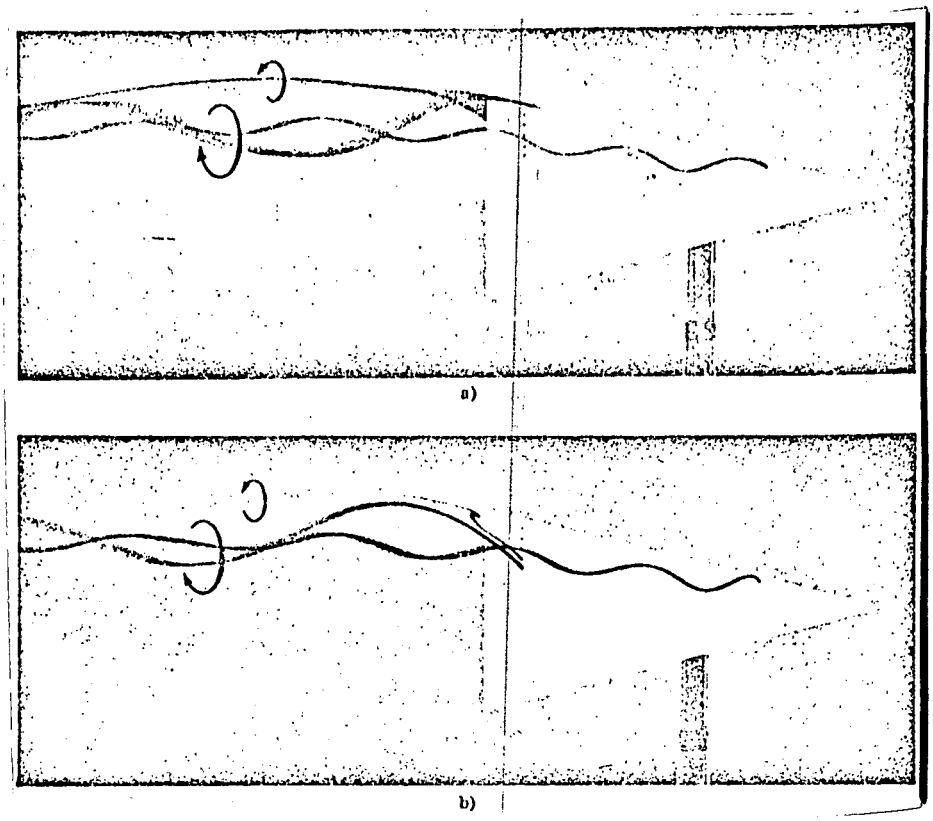

Fig. 11. Flow at the trailing edge of a delta wing of aspect ratio A = 1.0 at angle of attack α = 15°. a) Dye injected at lower side. b) Dye injected at upper side.

When flow on the upper side of the wing is made visible as shown in Fig. 11 b, the momentum of the dye exiting from the wing at the first hole (as reckoned from the center of the wing) is so high that a flow line somewhat distant from the wing is thereby colored. This dye filament therefore spirals into the leading-edge vortex. The dye injected from the second hole, with less momentum, enters the trailing-edge vortex sheet and thus the trailing-edge vortex, however. The further behavior of the /287
trailing-edge vortex downstream from the wing is primarily determined by the principal vortex. Fig. 12 shows flow about the delta wing of aspect ratio A = 1.0 at angle of attack α = 15° in horizontal and vertical views. Vortex formation is made visible here by a single dye filament which exits from the wing

surface at high momentum. On the one hand, the principal vortex is thereby made visible as a spiral of small amplitude. On the other hand, however, dye also reaches the immediate vicinity of the trailing edge, so the vortex sheet originating at the trailing edge is also dyed, with the trailing edge vortex.

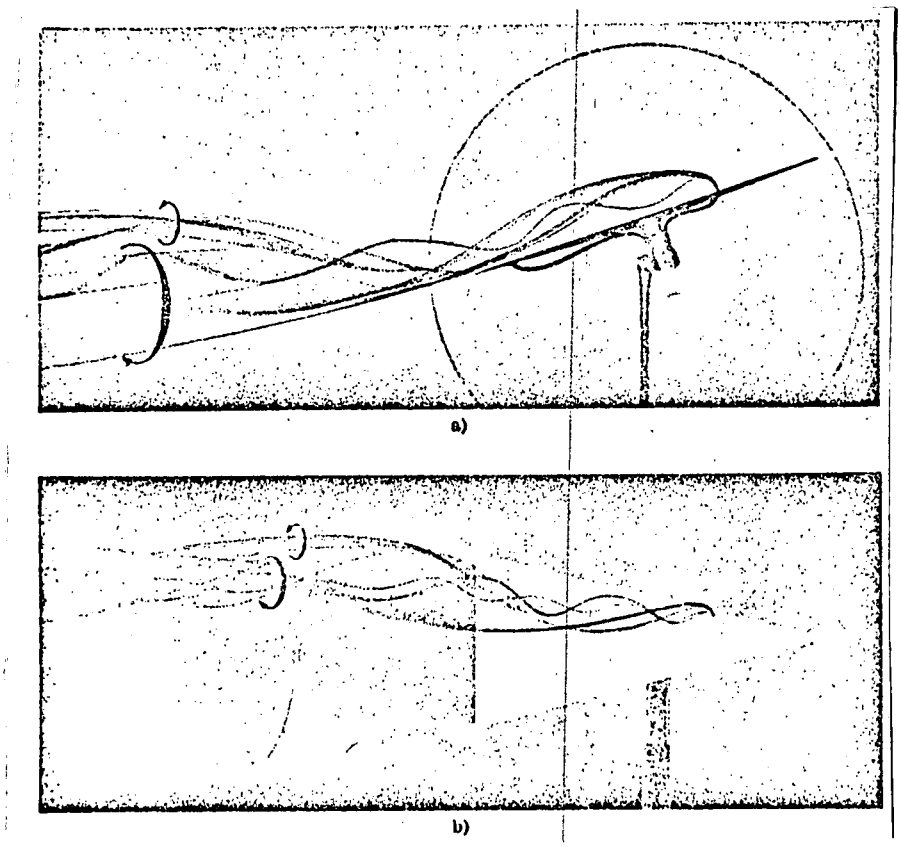

Fig. 12. Vortex formation behind a delta wing of aspect ratio A = 1.0 at angle of attack $\alpha = 15°$. a) Elevation, b) Overhead view.

The trailing-edge vortex leaves the wing approximately as an extension of the leading edge. Farther downstream, it bends in the direction of the free stream in the overhead view, whereas in the elevation, a pronounced upward displacement can be seen. The trailing edge vortex apparently behaves, under the influence of the velocities induced by the principal vortex, like a flow line in the principal vortex, spiraling about the axis of the principal vortex. Fig. 12 shows half a rotation by the trailing-

edge vortex about the principal vortex; at the left edge of the figure, the trailing-edge vortex lies above the principal vortex. Fig. 13 provides a schematic representation of these conditions. /288

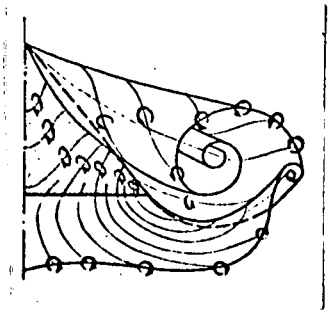

Fig. 13. Vortex formation behind a positioned delta wing (schematic).

5.3. Secondary Vortex and Trailing-Edge Vortex

It is reasonable to suspect that the trailing-edge vortex is connected with the secondary vortex resulting from boundary-layer separation on the suction side of the wing (cf. Section 4.2) or even represents a continuation of this secondary vortex downstream from the trailing edge. Both vortices rotate in the same direction. In order to study these relationships, flow in the secondary vortex was made visible. The results are shown in Fig. 14. A dye filament of low momentum was introduced directly into the secondary vortex through an opening in the wing surface close to the leading edge. In the forward area of the wing, secondary separation is well-ordered. At $x/\ell_i \sim 0.5$, however, phenomena occur which are reminiscent of the "bursting open" of the leading-edge vortex [13]: The secondary vortex widens (a portion of the dye enters the vortex sheet of the principal vortex), and reverse flow apparently occurs within the secondary vortex, since the dye in the secondary vortex, injected near the trailing edge on the suction side of the wing, flows toward the nose of the wing from the trailing edge. According to Fig. 14, the secondary vortex is not connected with the trailing edge vortex. The two are apparently of quite different natures: The secondary vortex represents a boundary-layer separation phenomenon, whereas the trailing-edge vortex is primarily a potential-theory effect which results from the behavior of the bound vortex lines on the lifting surface in the vicinity of the trailing edge.

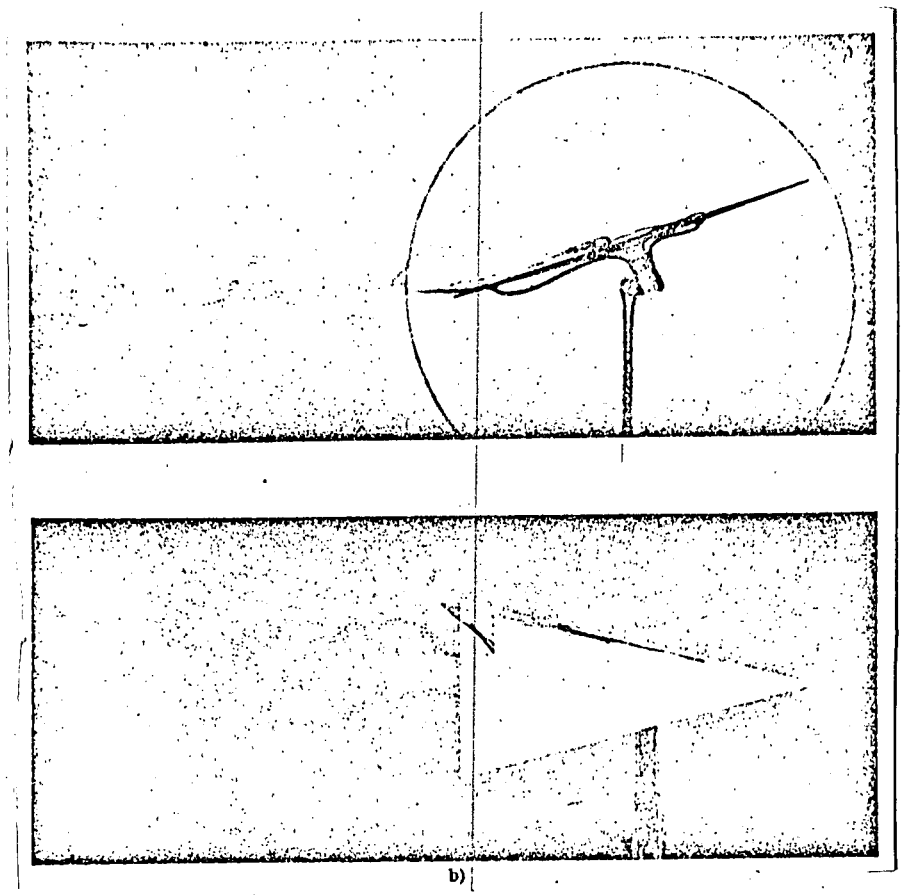

Fig. 14. Secondary-vortex formation on a delta wing of aspect ratio A = 1.0 at angle of attack α = 15°. a) Elevation, b) Overhead view.

6. Summary

Boundary-layer measurements were carried out on a slender, sharp-edged delta wing of aspect ratio A = 1.0 at angle of attack of α = 20.5° (C_L = 0.72). Artificially turbulent boundary layers were generated on the suction side of the wing. The paths of bound vortex lines on the lifting surface were determined from velocities at the margin of the boundary layers on the upper and lower sides. A comparison with earlier results from measurements /289 with laminar boundary layers [12] indicates that, depending on the state of flow, considerable differences exist in the v-components and in pressure distribution over the suction side within the vicinity of the pressure minimum, whereas the paths of vortex

lines are only slightly dependent upon the state of the suction-side boundary layer.

Studies on the behavior of flow downstream from the trailing edge indicated that the vortex sheet originating at the trailing edge rolls into a vortex whose direction of rotation is opposite to that of the leading-edge vortex on the same side of the wing. This so-called trailing-edge vortex occurs in the span direction, at the end of the wing. Its axis passes downstream as a spiral about the axis of the leading-edge vortex. The trailing-edge vortex does not represent a continuation of the secondary vortex.

REFERENCES

1. Schlichting, H. and Truckenbrodt, E., Aerodynamik des Flugzeuges [Aircraft Aerodynamics], Vols. 1 and 2, second edition, 1967 and 1969, Springer-Verlag, Berlin/ /Heidelberg/New York.

2. Brown, C. E. and Michael, W. H., "Effects of leading-edge separation on the lift of a delta wing," J. Aeronaut. Sci. 21, 690-694 (1954); see also NACA TN 3430 (1955).

3. Mangler, K. W. and Smith, J. H. B., "A theory of the flow past a slender delta wing with leading-edge separation," Proc. Roy. Soc. A 251, 200-217 (1959); see also RAE TN 2593 (1957).

4. Smith, J. H. B., "Improved calculations of leading-edge separation from slender delta wings," RAE TR 66 070 (1966).

5. Küchemann, D., "A nonlinear lifting surface theory for wings of small aspect ratio with leading-edge separation," RAE Report Aero 2540 (1955).

6. Gersten, K., "Nonlinear airfoil theory, particularly for airfoils of small aspect ratio," (Habilitation thesis, Technische Universität Braunschweig, 1960), Ing. Archiv 30, 431-452 (1961).

7. Nangia, R. K. and Hancock, G. N., "A theoretical investigation for delta wings with leading-edge separation at low speeds," Report from Queen Mary College, University of London, ARC 30 608 (F.M. 3994, S.C. 4229, L.D. 30), 1968.

8. Marsden, D. J., Simpson, R. W., and Rainbird, W. J., "The flow over delta wings at low speeds with leading-edge separation," College of Aeronautics, Cranfield, Rep. 114 (1958).

9. Peckham, D. H., "Low-speed wind-tunnel tests on a series of uncambered slender pointed wings with sharp edges," ARC Rep. Mem. 3186 (1961).

10. Hummel, D., "Experimental study of flow on the suction side of a slender delta wing," ZFW 13, 247-252 (1965).

11. Elle, B. J., and Jones, J. P., "A note on the vorticity distribution on the surface of slender delta wings with leading-edge separation," J. Roy. Aeronaut. Soc. 65, 195-198 (1961).

12. Hummel, D., "Flow about slender sharp-edged delta wings at high angles of attack," ZFW 15, 376-385 (1967).

13. Hummel, D., "Studies on the 'bursting apart' of vortices on slender delta wings," ZFW 13, 158-168 (1965).

14. Jones, R. T., "Properties of low-aspect-ratio pointed wings at speeds below and above the speed of sound," NACA Rep. 835 (1946).

15. Hummel, D. and Redeker, G., "The effect of the 'bursting apart' of vortices on the aerodynamic coefficients of delta wings of low aspect ratio in side-slip," Jahrbuch 1967 der WGLR, 232-240 (1968).